ARTICLE OPEN ACCESS

Autoimmune gait disturbance accompanying adaptor protein-3B2-IgG

Josephe A. Honorat, MD, PhD, A. Sebastian Lopez-Chiriboga, MD, Thomas J. Kryzer, AS, Lars Komorowski, PhD, Madeleine Scharf, PhD, Shannon R. Hinson, PhD, Vanda A. Lennon, MD, PhD, Sean J. Pittock, MD, Christopher J. Klein, MD, and Andrew McKeon, MD

Correspondence
Dr. McKeon
mckeon.andrew@mayo.edu

Neurology® 2019;93:e954-e963. doi:10.1212/WNL.0000000000008061

Abstract

Objective

To describe phenotypes, treatment response, and outcomes of autoimmunity targeting a synaptic vesicle coat protein, the neuronal (B2) form of adaptor protein–3 (AP3).

Methods

Archived serum and CSF specimens (from 616,025 screened) harboring unclassified synaptic antibodies mimicking amphiphysin–immunoglobulin G (IgG) on tissue-based indirect immunofluorescence assay (IFA) were re-evaluated for novel IgG staining patterns. Autoantigens were identified by western blot and mass spectrometry. Recombinant western blot and cell-binding assay (CBA) were used to confirm antigen specificity. Clinical data were obtained retrospectively.

Results

Serum (10) and CSF (6) specimens of 10 patients produced identical IFA staining patterns throughout mouse nervous system tissues, most prominently in cerebellum (Purkinje neuronal perikarya, granular layer synapses, and dentate regions), spinal cord gray matter, dorsal root ganglia, and sympathetic ganglia. The antigen revealed by mass spectrometry analysis and confirmed by recombinant assays (western blot and CBA) was AP3B2 in all. Of 10 seropositive patients, 6 were women; median symptom onset age was 42 years (range 24–58). Clinical information was available for 9 patients, all with subacute onset and rapidly progressive gait ataxia. Neurologic manifestations were myeloneuropathy (3), peripheral sensory neuropathy (2), cerebellar ataxia (2), and spinocerebellar ataxia (2). Five patients received immunotherapy; none improved, but they did not worsen over the follow-up period (median 36 months; range 3–94). Two patients (both with cancer) died. One of 50 control sera was positive by western blot only (but not by IFA or CBA).

Conclusion

AP3B2 (previously named β-neuronal adaptin-like protein) autoimmunity appears rare, is accompanied by ataxia (sensory or cerebellar), and is potentially treatable.

From the Departments of Laboratory Medicine and Pathology (J.A.H., T.J.K., S.R.H., V.A.L., S.J.P., C.J.K., A.M.), Neurology (A.S.L.-C., V.A.L., S.J.P., C.J.K., A.M.), and Immunology (V.A.L.), College of Medicine, Mayo Clinic, Rochester, MN; and Euroimmun, AG (L.K., M.S.), Lubeck, Germany.

Go to Neurology.org/N for full disclosures. Funding information and disclosures deemed relevant by the authors, if any, are provided at the end of the article.

The Article Processing Charge was funded by Mayo Clinic.

Glossary

ANNA-1 = autoimmunity and antineuronal nuclear antibody type 1; **AP3B2** = adaptor protein 3, subunit B2; **CBA** = cell-binding assay; **FITC** = fluorescein isothiocyanate; **HBSS** = Hanks Balanced Salt Solution; **IFA** = immunofluorescence assay; **IgG** = immunoglobulin G; **NGS** = normal goat serum; **PBS** = phosphate-buffered saline; **TRITC** = tetramethylrhodamine isothiocyanate; **ZnT3** = zinc transporter 3.

Some well-characterized autoimmune neurologic disorders have diverse manifestations, consistent with multifocal expression of the neural autoantigen throughout the central, peripheral, and autonomic nervous systems.[1] For example, patients with paraneoplastic neurologic autoimmunity and antineuronal nuclear antibody type 1 (ANNA-1, also known as anti-Hu) may present with peripheral neuropathy (classically, but not exclusively, sensory neuronopathy), ataxia, myelopathy, dysautonomia, encephalopathy, or mixed manifestations.[2,3] We describe an autoimmune disorder unified by gait instability–predominant neurologic presentation. All patients had ataxia (one or other of cerebellar, dorsal column, or sensory neuronal dysfunction) and adaptor protein 3, subunit B2 (AP3B2) immunoglobulin G (IgG) detected in serum and CSF. Twenty-seven years ago, this autoantibody was described in a single patient with autoimmune cerebellar ataxia and was named anti-Nb IgG.[4]

Methods

Standard protocol approvals, registrations, and patient consents

The Mayo Clinic Institutional Review Board approved human specimen acquisition and retrospective review of patients' histories (IRB# 16–009814).

Study population

Between January 1, 1993, and April 30, 2017, the Mayo Clinic Neuroimmunology Laboratory tested by tissue-based indirect immunofluorescence assay (IFA), on a service basis, 616,025 serum and CSF specimens submitted for patients undergoing workup for a suspected paraneoplastic neurologic or autoimmune encephalitic illness. Of those specimens, 367 (serum, 334; CSF, 34) revealed a pattern of diffuse neural synaptic (neuropil) staining resembling (but not meeting criteria for) amphiphysin IgG, and were recorded as such in our archival records. All 367 specimens were retested by IFA and classified in detail according to their respective IgG staining patterns.[5] Among those were 10 patients with an identical staining pattern, which is the subject of this report. Clinical information (available in 9 patients) was obtained by review of Mayo Clinic records (4) and from external physicians by telephone interview in the course of clinical consultation with our laboratory (5). Of those 5, additional information was obtained during the course of the study in 3.

Indirect IFA and dual staining by confocal microscopy

Patient sera (1:240) and CSF (1:2) were tested on cryosections of composite adult mouse tissues: cerebellum, midbrain, cerebral cortex, hippocampus, kidney, and gut, as described previously.[6] For dual staining of mouse tissue, the AP3B2 rabbit polyclonal IgG (1:50–1:100 reactive with polypeptide 650–1,082, Proteintech, Rosemont, IL) was used. Secondary antibodies were fluorescein isothiocyanate (FITC)–conjugated anti-human (1:200) and tetramethylrhodamine isothiocyanate (TRITC)–conjugated anti-rabbit IgG (1:200, SouthernBiotech, Birmingham, AL). Confocal images were captured using a microscope (×20 and ×40 water immersion lenses, LSM780; Carl Zeiss AG, Oberkochen, Germany).

Hippocampal neuron preparation

Rat hippocampi were dissected from E18–20 animals and meninges were removed. Tissue was minced in Hanks Balanced Salt Solution (*HBSS*). Minced tissue was incubated in 4.5 mL HBSS with 0.5 mL 0.25% trypsin in a 37°C water bath for 15 minutes with gentle inversion every 5 minutes. Tissue was washed with HBSS +10% fetal bovine serum with DNAse at 37°C for 5 minutes. After washing 2 more times in HBSS at 37°C, tissue was triturated in HBSS. Larger tissue chunks were allowed to settle and the supernatant was transferred to new tubes. Trituration was repeated and supernatants were combined. Cells were counted and plated at 5×10^4 in Neural Basal plus media with B27 supplement (Gibco, Gaithersburg, MD) and held at 37°C in a humidified atmosphere of 9% air/% CO_2. Fresh medium was exchanged for half the spent medium volume every 4 days.

Live hippocampal neuron immunofluorescence

Six to ten days before the assay, neurons were subcultured on laminin/poly-L-lysine-coated glass coverslips (MatTek, Ashland, MA) at $\times 10^4$. Steps thereafter were performed at 4°C. After washing with phosphate-buffered saline (PBS), neurons were exposed for 30 minutes to patient samples (all 10 sera or 4 available CSFs) diluted in 10% normal goat serum (NGS) at 1:5 or undiluted, respectively. Control specimens were CSF from a patient with NMDAR encephalitis,[7] serum from a healthy participant, and CSF from a patient with normal pressure hydrocephalus. Cells were washed in PBS and exposed for 30 minutes to FITC-conjugated goat anti-human IgG secondary antibody (SouthernBiotech) diluted in 10% NGS. Cells were washed in PBS and exposed to 4% paraformaldehyde at room temperature, 15 minutes. To label axons, cells were permeabilized in 0.2% Triton X-100 for 10 minutes, washed in PBS, then exposed sequentially to 10% NGS for 30 minutes, and mouse anti-acetylated tubulin IgG (Sigma-Aldrich [St. Louis, MO], diluted 1:500 in 10% NGS

for 16 hours at 4°C). Cells were washed, probed with TRITC-conjugated goat anti-mouse IgG, washed in PBS, and mounted in Prolong Gold with DAPI (Invitrogen, Carlsbad, CA). Confocal images were captured using a Zeiss LSM710 confocal microscope with ×40 water immersion lens.

Western blot

For western blots, a mouse cytosolic cerebellar extract was separated on 4%–15% polyacrylamide gels, transblotted to nitrocellulose membranes, and probed with IgGs from healthy controls or patients (1:400 dilution), or commercial AP3B2-specific IgG (1:5,000). The recombinant AP3B2 polypeptide (human protein residues 650–1,082; ~73 kDa) used to confirm antigen specificity (Proteintech) includes the AP3B2 C-terminal region, which was originally demonstrated to include the pertinent autoantigen.[8] We evaluated sera from all patients and 10 healthy controls.

Protein purification and sequencing by mass spectrometry

Serum IgGs from 3 patients (2, 4, and 8) and 1 healthy control were complexed to protein G magnetic beads (Dynabeads; Invitrogen, Thermo Fisher Scientific [Waltham, MA]) and exposed to mouse cerebral or cerebellar protein extract (20 minutes, at room temperature). After washing, beads were boiled for 5 minutes in 2 × Laemmli sample buffer. The eluted proteins were electrophoresed in 5% polyacrylamide gel, and located by Coomassie G-250 staining (Bio-Rad, Hercules, CA) and by western blot. Bands corresponding to immunoreactivity were excised and analyzed by high-pressure liquid chromatography electrospray tandem mass spectrometry (Mayo Clinic Medical Genome Facility—Proteomics Core).

Cell-binding assay (CBA)

AP3B2 specificity was confirmed by indirect immunofluorescence on HEK293 cells transfected with full-length AP3B2 isoform 1 complementary DNA (SWISSPROT #Q13367). Control cells were transfected with empty vector. Cells were grown on glass coverslips, fixed with ice-cold acetone, and prepared as millimeter-sized biochip fragments on microscope slides as a mosaic of AP3B2-expressing and control cells (Euroimmun AG, Lübeck, Germany).

Controls tested

Serum controls tested by indirect IFA (564 total) were from 317 healthy controls, 94 Mayo Clinic patients with suspected paraneoplastic disorders and N-type calcium channel antibody positivity (2011–2013),[9] 63 cancer patients without neurologic disease, and 90 patients with other neurologic diseases (Creutzfeldt-Jakob disease [30], CNS systemic lupus erythematous [10], multiple sclerosis [20], and amyotrophic lateral sclerosis [30]). Sera tested by AP3B2-IgG western blot were 30 healthy and 20 with ≥1 other paraneoplastic antibodies (Purkinje cell cytoplasmic antibody type 1 [PCA-1, anti-Yo], 10; ANNA-1, 10). Specimens tested by AP3B2-IgG CBA were 20 healthy and 13 with ≥1 other paraneoplastic antibodies (PCA-1, 7; ANNA-1, 6).

Data availability

All data pertaining to this article are contained within or published as online supplement.

Results

Characterization of the autoantigen

Immunohistochemical distribution of the neural antigen

Indirect IFA of 10 patients' serum (10) and CSF specimens (6), using cryosections of murine brain and gut tissues, demonstrated an identical staining pattern in each (figure 1, A–D). Patient IgGs reacted diffusely with perikarya of Purkinje neurons and myenteric plexus, cerebellar granular layer synapses, and dentate regions, and could be distinguished from other synaptic neural IgGs (table). No staining was detected in the parenchyma of kidney or gut (not shown).

Prominent reactivity was also observed in the spinal cord (particularly in the dorsal horn; figure 1E), most striking of all, in paraspinal ganglia (dorsal root and sympathetic) and to a lesser extent in the dorsal root (figure 1, F and G).

Identification and confirmation of AP3B2 as antigen

Immunoblotting of mouse cerebellar lysates with patients' serum, but not healthy control serum, revealed a common immunoreactive band of interest with approximate molecular weight of 150 kDa (figure 1H). To identify the target antigen, immunoprecipitation of mouse cerebellar extract was performed using sera from patients 2, 4, and 8. Mass spectrometry analysis of the electrophoretically separated proteins identified AP3B2 as the 150 kDa protein. AP3B2 (previously known as β-neuronal adaptin-like protein) was reported in 1991 as the target antigen in a single case of autoimmune cerebellar ataxia.[4]

None of patient sera 1–10, or 4 available CSF, demonstrated IgG binding to live hippocampal neurons (figure 2). In contrast, CSF from the NMDAR-positive patient bound strongly to live neurons. Sera from patients 1–10 demonstrated strong immunoreactivity with both a 73 kDa recombinant AP3B2 polypeptide fragment (residues 650–1,082) and the AP3B2 CBA (reactive with AP3B2-transfected cells, but not mock-transfected cells) (figure 3, A and B). Available CSF specimens from patients 1, 5, and 7 were also tested by the CBA and were positive. All 470 controls tested by IFA were negative. One of 50 control sera (from a healthy participant) tested by recombinant AP3B2 western blot was positive, but subsequently proved negative by IFA and CBA. IFA demonstrated colocalization of commercial AP3B2 IgG and patient IgG on mouse brain tissue (figure 3C).

Serologic results

Of 10 patients, 9 were identified retrospectively from the Mayo Clinic Neuroimmunology Laboratory archives (from 1997 to 2015) and 1 patient was identified prospectively after

Figure 1 Distribution of adaptor protein 3, subunit B2 immunoreactivity in mouse tissues revealed by patient immunoglobulin G (IgG) binding

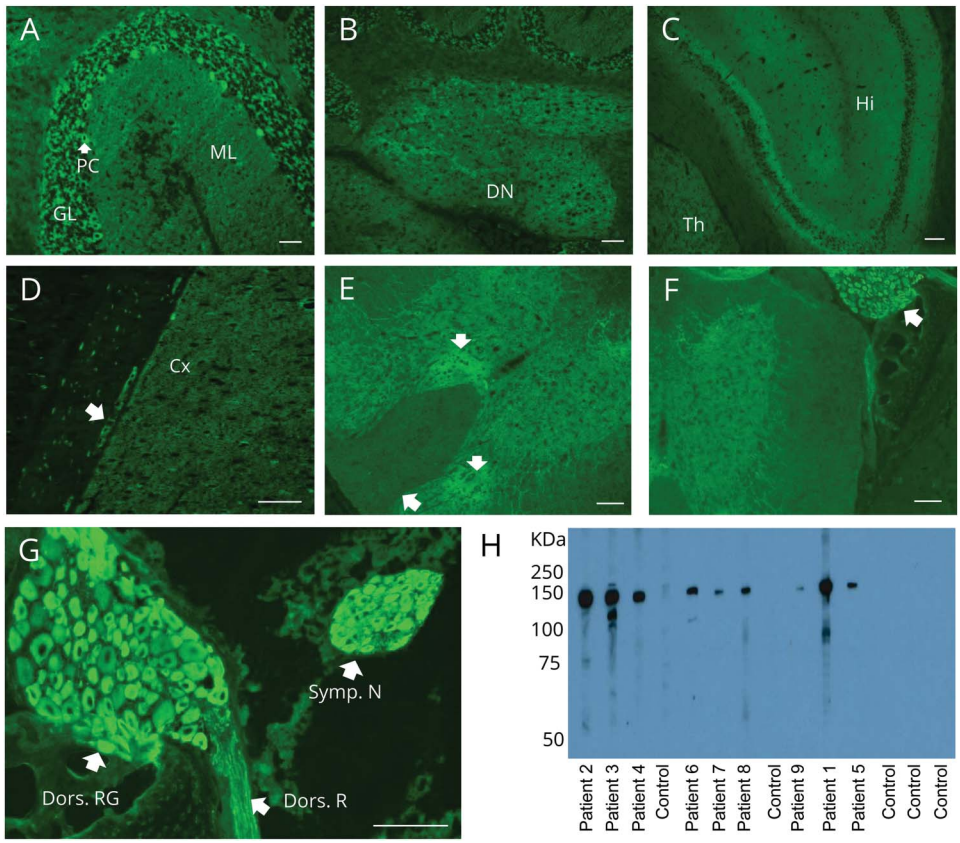

(A–G) Patient serum IgG yields synaptic pattern of immunofluorescence in (A) cerebellar granular layer (GL) more than molecular layer (ML), plus perikarya of Purkinje cells (PC); (B) cerebellar dentate nucleus (DN); (C) hippocampus (Hi), thalamus (Th); (D) cerebral cortex (Cx) and ganglionic neuronal perikarya in juxtaposed gastric smooth muscle (arrow); and (E) spinal cord gray matter (particularly dorsal regions [arrows]). (F, G) Immunoreactivity is most prominent in perikarya of dorsal root (F, enlarged in G) and sympathetic ganglionic neurons and dorsal root nerve fibers (G). (H) In western blot, cytosolic lysate of mouse cerebellum contains a prominent antigenic protein of approximately 150 kDa, reactive with IgG in sera of patients 1–9, but not with healthy control sera IgG. Scale bar: A, B, D, 50 μm; C, E–G: 100 μm.

the study was underway. IFA endpoint dilutions were 1:30,720 in serum (range 3,840–61,440) and 1:64 in CSF (range 32–256). N-type voltage-gated calcium channel antibody coexisted in sera of 8 of 10 patients with a median value of 0.07 (range 0.04–0.15; normal ≤0.03 nmol/L), and 2 patients had low titer GAD65 antibody detected (0.17, 0.03 nmol/L; normal ≤0.02 nmol/L, table).

Summary of demographic and clinical findings

Six of ten patients were women. The median age at symptom onset was 42 years (range 24–58).

Neurologic manifestations

Clinical information was available in 9 of 10 patients (all but patient 2). The median follow-up period was 36 months (range 3–94). Symptom onset was subacute and rapidly progressive over weeks in all 9 patients. Syndromic manifestations of AP3B2 autoimmunity were myeloneuropathy, 3; peripheral sensory neuronopathy, 2; cerebellar ataxia, 2; and spinocerebellar ataxia, 2 (table).

All 9 patients reported gait disturbances, accompanying sensory ataxia in 5 and cerebellar ataxia in 4. In patients with cerebellar disorders, other presenting symptoms included dysarthria, 4; vertigo, 4; dizziness, 2 and tremor, 1. In patients with neuropathy or myeloneuropathy, other presenting symptoms included paresthesias, weakness, or numbness (2 each). Two patients had autonomic dysfunction affecting gastrointestinal motility, 2, or bladder, 1.

Cerebellar signs included ataxic gait, 4; nystagmus, 4; dysmetria, 4, and dysdiadochokinesia, 3. Among patients with neuropathy, sensory ataxic gait was present in 3, flaccid paraplegia in 1, areflexia or hyporeflexia in 3, and distal distribution loss of pinprick, vibration, and temperature in 5. Two patients with cerebellar ataxia had areflexia of the lower extremities and bilateral Babinski signs. The patient with myeloneuropathy had hyperreflexia of the lower extremities and unilateral Babinski sign.

Oncologic and autoimmune accompaniments

One of 9 patients had renal cell carcinoma detected prospectively. AP3B2 immunoreactivity was not detected in neoplasm sections. An additional patient had a history of B-cell lymphoma. Both patients died. Coexisting autoimmune disorders included Sjögren syndrome, 1; systemic sclerosis, 1; and hypothyroidism, 1.

CSF studies

CSF analysis data were available for 6 of 9 patients; all were abnormal. Four had elevated white cell count (median

Table Demographic, clinical, and paraclinical data for adaptor protein 3, subunit B2–immunoglobulin G–positive patients

Patient no./sex, y/age/race[a]	Main neurologic symptoms and signs	Neurologic diagnosis	Other diagnoses and neural autoantibodies	CSF abnormalities	Neuroimaging/electrophysiologic findings	Immunotherapy (improvement)	mRS, last follow-up	Disease duration, onset to last follow-up or death, mo
1/F/29/Caucasian[b]	Balance difficulty, dysarthria, ataxia, tremor, dizziness, vertigo	Cerebellar ataxia	Hypothyroidism	TNC: 7 (95% lymphocytes).	MRI brain: cerebellar atrophy prominent in vermis	NA	4	7
3/F/58/Caucasian[b]	Paresthesia, gait ataxia, balance difficulty, bilateral lower extremity weakness, bladder urgency and incontinence, constipation	Myeloneuropathy, dysautonomia	Renal cell carcinoma; VGCC-N, 0.04 nmol/L	6 OCB, protein 87 mg/dL	MRI brain: normal; MRI cord: cord atrophy, dorsal LETM; EMG: severe polyradiculopathy affecting thoracic and lumbosacral segments	IVMP, PLEX, IVIg, IV cyclophosphamide (none)	6	60 (died)
4/F/24/NA	Sensory ataxia, weakness, gastroparesis	Sensory neuropathy, dysautonomia	VGCC-N, 0.15 nmol/L	TNC, 6	EMG: sensory neuropathy	IVMP, IVIg (none)	3	36
5/F/30/Caucasian[b]	Right hand numbness, paresthesiae, dizziness, vertigo	Myeloneuropathy	Sjögren syndrome; VGCC-N, 0.07 nmol/L	TNC, 7 (93% lymphocytes), no OCB, protein normal	MRI cord: tractopathy (T2 signal in posterior columns); EMG: diffuse large fiber sensory neuropathy	IVIg, rituximab, mycophenolate mofetil (none)	2	94
6/M/44/NA	Myalgia, neuropathy	Sensory neuropathy	Remote B lymphoma; VGCC-N, 0.14 nmol/L	NA	NA	NA	6	30 (died)
7/F/40/NA	Gait disturbance	Myeloneuropathy	VGCC-N, 0.06 nmol/L	NA	MRI cord: spinal cord atrophy; EMG: sensory predominant neuropathy	PLEX, IVIg (none)	4	48
8/M/43/NA	Progressive ataxia, dysarthria	Cerebellar ataxia	VGCC-N, 0.07 nmol/L	TNC, 8 (lymphocytic), supernumerary OCBs, protein 39 mg/dL	MRI brain: moderate cerebellar atrophy	NA	4	3
9/F/42/Caucasian[b]	Gait disturbance, incoordination, dysarthria, coordination difficulty	Spinocerebellar syndrome	VGCC-N, 0.37 nmol/L; GAD65, 0.17 nmol/L	Protein, 46 mg/dL	MRI brain: cerebellar atrophy; MRI cord: normal; EMG: normal	IVMP, PLEX, IVIg (none)	4	40
10/M/43/NA	Ataxia, dysarthria, severe vertigo	Spinocerebellar syndrome	VGCC-N, 0.07 nmol/L; GAD65, 0.03 nmol/L	NA	MRI brain: cerebellar atrophy	NA	NA	NA

Abbreviations: GAD65 = glutamic acid decarboxylase 65 kDa isoform; IVIg = IV immunoglobulin; IVMP = IV methylprednisolone; LETM = longitudinally extensive transverse myelitis; mRS = modified Rankin Scale score; NA = not available; OCB = oligoclonal bands; PLEX = plasma exchange; TNC = total nucleated cell count; VGCC-N = N-type voltage-gated calcium channel.

[a] Patient 2 had no clinical information available.

[b] Patients evaluated in the Department of Neurology, Mayo Clinic, underwent extensive evaluations for alternative causes, all of which were negative. Testing including serum ceruloplasmin or copper and B_{12} in all patients (all normal) and EMG studies in 3 (none had evidence of Lambert-Eaton syndrome).

Figure 2 Live cell binding of control and patient immunoglobulin G (IgG) on hippocampal neurons

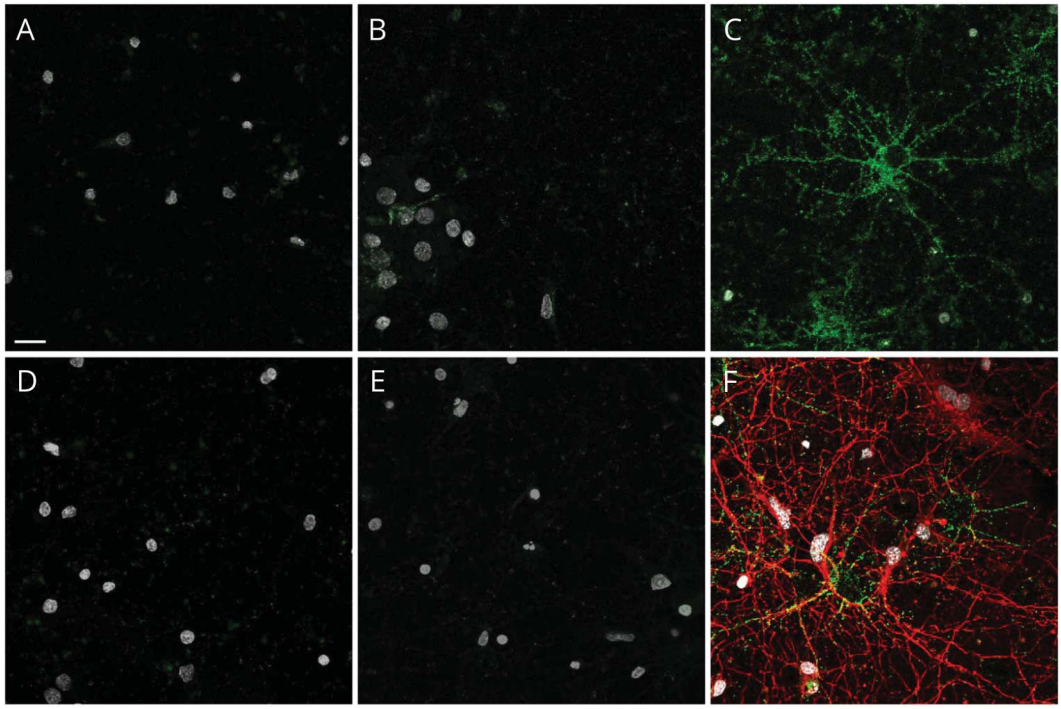

(A) Control CSF from normal pressure hydrocephalus patient and (B) healthy control serum do not bind to the surface of living hippocampal neurons. Neither CSF (D) nor serum (E) from patients 1–10 (representative images from patient 5) bind to the neuronal cultures. In contrast, NMDAR-IgG-positive patient CSF binds in a punctate pattern to the extracellular surface of hippocampal neurons (C, green). Cells were poststained for acetylated tubulin to identify axons (F, red). Nuclei stained with DAPI in all panels (white). Scale bar, 20 μm.

value 7/μL; range 6–8 [normal ≤5]), 3 had elevated protein (median value 46 mg/dL; range 39–87 mg/dL [normal ≤ 35 mg/dL]), 1 had an increased IgG index and synthesis rate, and 2 had elevated CSF-exclusive oligoclonal band numbers (table).

Imaging and electrophysiology

Brain MRI revealed cerebellar atrophy in all 4 patients with cerebellar ataxia (figure 4, A.a and A.b). Bilateral T2 hyperintensities in the subcortical and periventricular white matter were also present in one of those patients (not shown). MRI spinal cord images were abnormal in 3 of 6 patients evaluated (all 3 had myeloneuropathy): cord atrophy and bilateral T2 hyperintensities within the central gray matter from T10 to T12 (patient 3; figure 4, B.a and B.b), longitudinally extensive T2 signal abnormality of the posterior columns (patient 5, figure 4, C.a and C.b), and prominent atrophy (patient 7, not shown). EMG revealed abnormal findings in 4 patients: diffuse large fiber sensory neuropathy in 2, sensory neuronopathy in 1, and severe polyradiculopathy of the thoracic and lumbosacral segments in the solitary patient with myeloneuropathy.

Neuropathology

Sural nerve biopsy tissue was obtained in patient 5 (with myeloneuropathy), 2 years after onset of symptoms. Teased peripheral nerve fiber preparation demonstrated increased empty nerve strands and axonal degeneration (figure 5A). Immunohistochemistry revealed CD68+ macrophage infiltration in the endoneurium (figure 5B). Multifocal loss of large and small myelinated fibers was consistent with neuron-directed cytotoxicity (figure 5, C and D).

Treatment and outcomes

Five of nine patients received one or more immunotherapies; none of them improved. Three did not worsen and two progressed despite treatment with multiple immunotherapies. Both patients with cancer died. At last follow-up, 2 patients were able to ambulate independently, 3 were using cane or walker, and 1 was wheelchair-bound. The median modified Rankin Scale score at last follow-up was 4 (range 2–6). Median duration from onset to last follow-up was 36 months (range 3–84).

Discussion

All 9 patients with clinical information available in whom we identified AP3B2-reactive IgG had a neurologic phenotype of gait dysfunction secondary to ataxia, either cerebellar or sensory, or a mixture of both. In addition, 2 patients had gastrointestinal dysautonomia. The clinical findings corresponded to the multifocal distribution of the patients' serum IgG immunoreactivity on murine neural tissues, being most prominent in cerebellar Purkinje neurons, dorsal spinal cord, dorsal root ganglia, and autonomic ganglia.[8] This distinctive

Figure 3 Western blot with recombinant protein and confocal microscopy confirm the target antigen is a cytosolic protein, adaptor protein 3, subunit B2 (AP3B2)

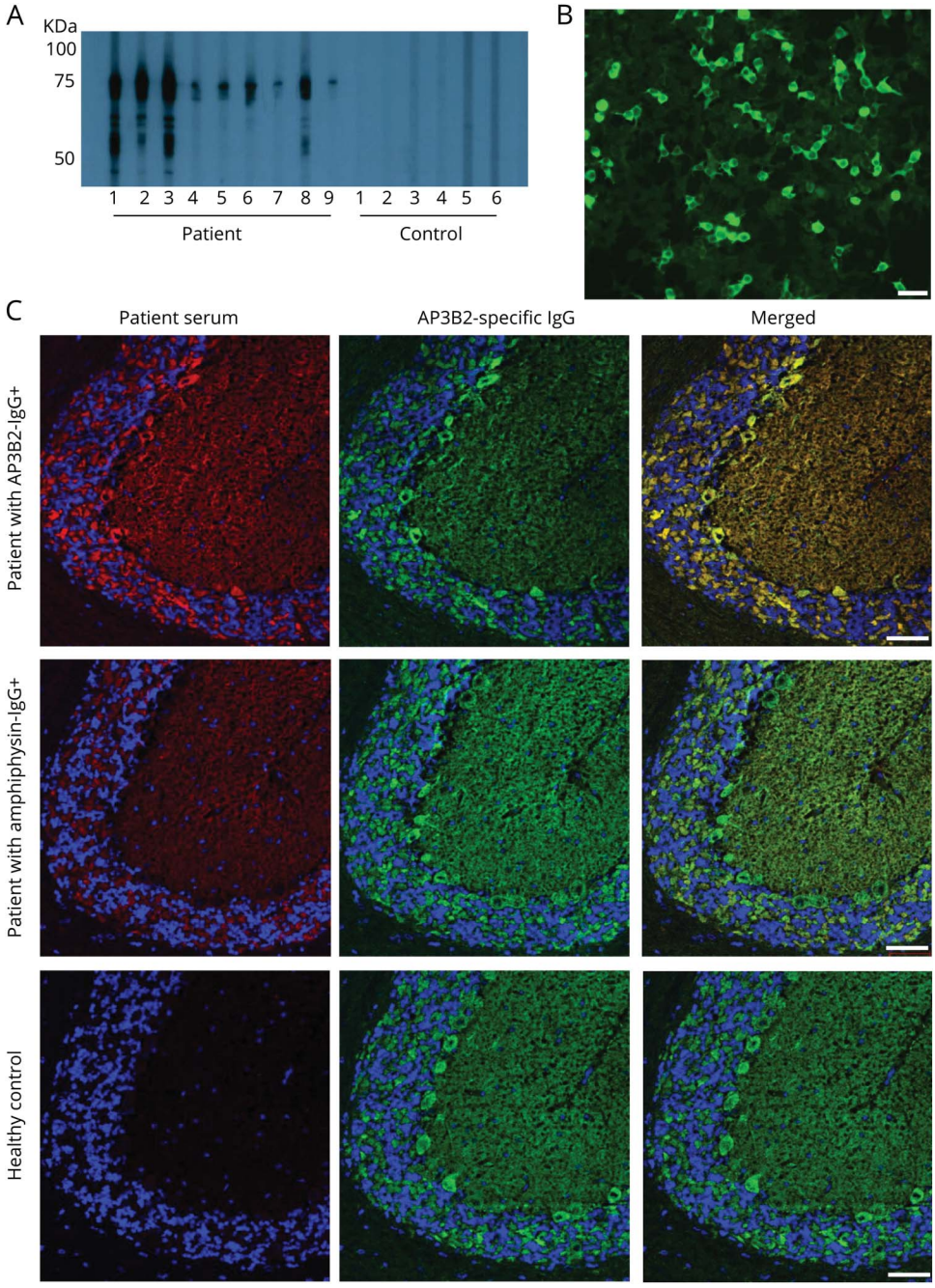

(A) By western blot, immunoglobulin G (IgG) from 9 patient sera, but none of 6 healthy control sera shown, bind to a recombinant AP3B2 C-terminal polypeptide fragment. (B) Positivity by AP3B2-specific cell-binding assay in serum of patient 7. (C) Commercial AP3B2 antibody colocalizes well with immunoreactivity produced on mouse cerebellum by patient AB3B2-IgG (top), but not with amphiphysin-IgG-positive patient (middle) or healthy control (bottom). Left column, patient IgG; middle column, rabbit anti-AP3B2 IgG; right column, merged images. Scale bars, 50 μm.

neuron-specific pattern of IgG staining unified the patients serologically. IgG in all patient specimens bound to a C-terminal polypeptide segment of the vesicle-coat protein-sorting adaptor protein complex, AP3B2, earlier identified as an autoantigen reactive with IgG in serum of a patient presenting with pancerebellar ataxia with diffuse hyperreflexia and bilateral plantar extensor responses.[4,8]

The spinal cord MRI of 2 of our seropositive patients demonstrated longitudinally extensive, symmetric, tract-restricted, T2-signal abnormalities that are the radiologic hallmark of tractopathies associated with certain autoimmune myelopathies, particularly paraneoplastic entities.[10] The subacute cerebellar syndrome reported in the original case of AP3B2 autoimmunity progressed rapidly, confining the patient to bed within 2 months.[4] Some of our patients had similar onset and progression of symptoms, with significant residual neurologic disability. However, 3 of 5 did not worsen after treatment (which could be due to treatment or natural history), and some had relatively long survival.

Figure 4 Brain and spinal cord MRI

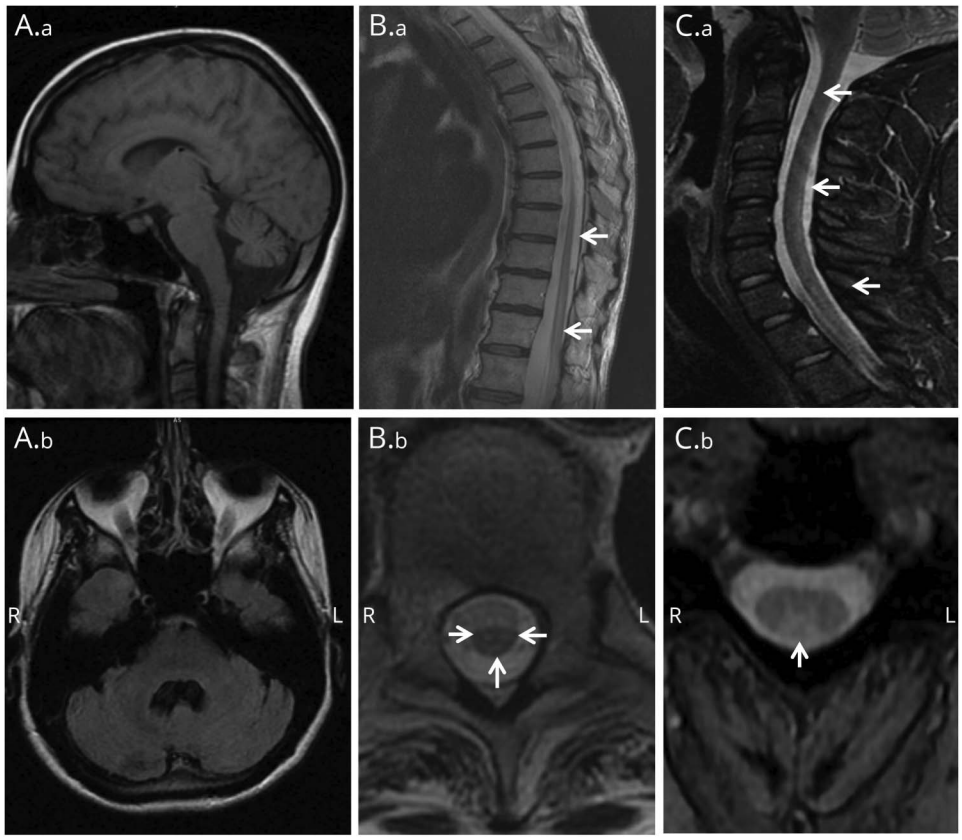

Patient 1: (A.a) Prominent cerebellar atrophy in sagittal T1-weighted brain MRI. (A.b) Enlarged IVth ventricle in axial T1-weighted brain MRI. Patient 3: (B.a) Longitudinal lesion extending from T9 to conus medullaris in sagittal T2-weighted thoracolumbar spine MRI. (B.b) Increased T2 signal in spinal cord gray matter and posterior columns (arrows) consistent with tractopathy (axial T2-weighted). Patient 5: (C.a, C.b) Increased T2 signal in spinal cord posterior columns (arrows) in sagittal (C.a) and axial (C.b) T2-weighted cervical spine MRI.

The index patient lacked detectable cancer, but a paraneoplastic cause was suspected on finding AP3B2 immunoreactivity in neuroectodermal neoplastic cell lines (melanoma, small-cell lung cancer and neuroblastoma).[4] Two of our patients had past or contemporaneous evidence of cancer (lymphoma and renal cell cancer, respectively), but a paraneoplastic etiology was uncertain. The renal cell carcinoma lacked detectable AP3B2 immunoreactivity, and the patient did not improve after tumor resection and extensive immunotherapy. She died, paraplegic, 7 years after the onset of neurologic symptoms. The ages of our patients (median 42 years) and of the patient previously reported (35 years) were notably younger than what is generally reported for paraneoplastic neurologic disorders (60–65 years).[3,11,12]

The composition and targeting of synaptic vesicles is determined by their cytosolic coat constituents. The clathrin-independent heterotetrameric AP3 protein is composed of beta, delta, mu, and sigma subunits.[13] AP3A is ubiquitous (expressed in nerve cell bodies) and directs proteins from endosomes to lysosomes.[14] The neuron-restricted AP3B2 isoform resides in dendrites and axons, and directs proteins from endosomes to synaptic vesicles.[8] As a biomarker, AP3B2 IgG aids the diagnosis of a discrete neurologic syndrome, but the cytosolic location of its antigen predicts that this autoantibody is not neuropathogenic per se, but rather a surrogate marker for CD8+ cytotoxic T cells targeting peptides derived from AP3B2.

Sera of all AP3B2-IgG-positive patients except 1 immunoprecipitated N-type ($Ca_v2.2$) voltage-gated calcium channels complexed with radioiodinated omega-conotoxin GVIA.[15] The apparent coexistence of 2 discrete neural autoantibodies suggests that $Ca_v2.2$ and AP3B2 may act as co-immunogens. Alternatively, the topographic localization of both the $Ca_v2.2$ channel and AP3B2 in nerve terminals suggests that co-immunoprecipitated $Ca_v2.2$ might represent a physiologic presynaptic complex between these molecules. An analogy can be drawn to the co-immunoprecipitation of detergent-solubilized K_v1 potassium channels with Lgi1 and CASPR2.[16,17] Two patients had low positive GAD65 antibody values, which are common in the general population, and do not have neurologic significance.

AP3-sorted proteins, such as zinc transporter 3 (ZnT3), are recognized by both AP3A and B2 isoforms, on the same endosomes, and are routed to either synaptic vesicular or lysosomal pathways, respectively.[18,19] In mice with homozygous deletion of the *AP3B2* gene, ZnT3 and other synaptic vesicle membrane proteins are directed exclusively to lysosomes for degradation. Electrophysiologically, those mice exhibit attenuation of the asynchronous release of

Figure 5 Whole sural nerve biopsy of patient 5 demonstrates multifocal axonal degeneration without evident inflammation

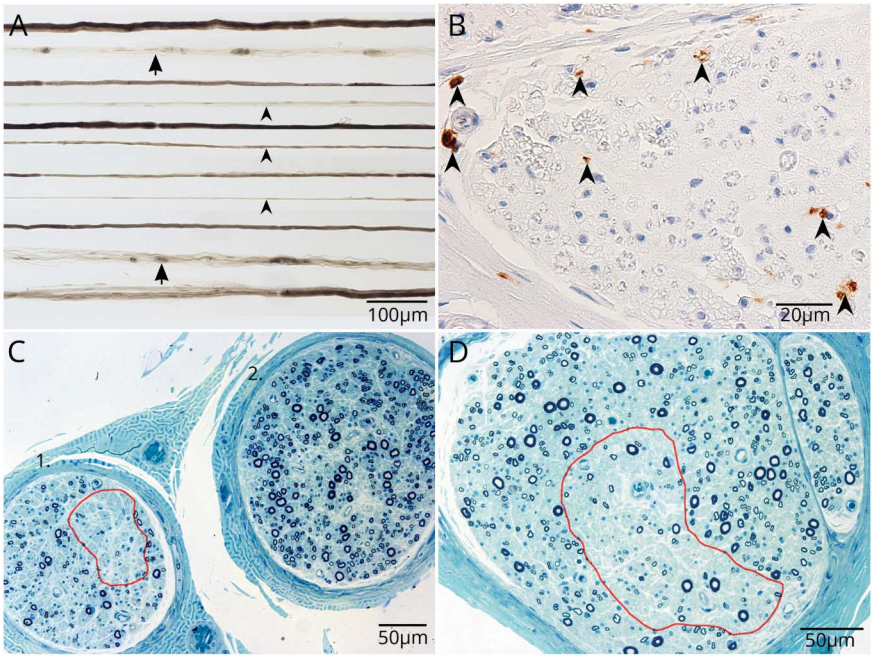

(A) Closely approximated teased nerve fibers stained with osmium tetroxide show increased empty nerve strands (arrowheads) and increased axonal degeneration (arrows). (B) Formalin-fixed paraffin section. CD68 immunoreactive cells are more numerous than normal; presumed macrophages, but lacking CD45 immunoreactivity. (C, D) Loss of axonal fibers is variable between fascicles and within fascicles (C, D, red outlined).

neurotransmitter that ensures precision of action potential firing.[20] Seven individuals with onset of epileptic encephalopathy and optic atrophy before 1 year of age and 5 with hypotonia and impaired motor development were reported to have autosomal recessive mutations in AP3B2.[21] In other children with Hirschsprung disease, an autonomic neuropathy of the colon, AP3B2 mutations have also been reported.[22] The gastrointestinal dysmotility noted in 2 of our patients may plausibly be attributed to AP3B2 autoimmunity.

Consistent with an exclusively cytosolic localization within synapses, none of our patients' IgGs demonstrated reactivity with extracellular domains of transmembrane proteins. However, AP3B2 IgG was detectable using a fixed and permeabilized AP3B2-specific cell line. Cytotoxic T lymphocytes, and not antibodies, are recognized to be the effectors of pathogenicity in autoimmune neurologic disorders defined by IgGs specific for intracellular neural antigens (e.g., CDR2 or HuD antigens of PCA-1 and ANNA-1 autoantibodies). Instead, CD8+ T-cell infiltration is the neuropathologic hallmark of those disorders, e.g., in the cerebellum of patients with ataxia associated with PCA-1 IgG and in dorsal root ganglia of patients with paraneoplastic sensory neuronopathy associated with ANNA-1 IgG.[12,23–25] Dorsal root ganglion tissue was not available from the AP3B2-IgG-positive patients we report with sensory ataxia. However, biopsied sural nerve from one patient demonstrated degenerative changes with focal axonal fiber loss, rather than inflammation. It is plausible that degenerative changes occurred in distal sensory nerves secondary to cytotoxic T-cell attack on dorsal root ganglia.

Ideally, testing for AP3B2 IgG would be incorporated in a diagnostic laboratory algorithm for evaluating patients with suspected autoimmune ataxia. For quality assurance, 2 steps are required for positivity. First, a tissue-based immunohistochemical screening assay permits simultaneous evaluation for multiple ataxia-pertinent autoantibodies (e.g., metabotropic glutamate receptor-1 IgG, as well as AP3B2 IgG). Second, a molecular reflex confirmatory step permits confirmation of the IFA finding. One of our 50 controls showed reactivity by western blot, but subsequent investigation revealed it was negative by IFA and CBA. Thus, utilization of an AP3B2-IgG-specific western blot in isolation might result in false-positives.

Autoimmunity targeting neuronal AP3B2 is an additional consideration for the differential diagnosis of patients presenting with mixed cerebellar and sensory ataxia and myeloneuropathy. Other potentially treatable entities must be excluded, such as ANNA-1 autoimmunity, Sjögren syndrome,[2,26] vitamin B_{12} deficiency (pernicious anemia) or other deficiencies of copper, zinc, folate, or vitamin E due to dietary deficiency, or malabsorptive enteropathy.[27]

Acknowledgment

The authors thank Jacquelyn Grell for assistance with live cell assay development; Yong Guo, MD, and Claudia Lucchinetti, MD, for assistance with tumor staining; and Neuroimmunology Laboratory staff for logistical and technical assistance.

Study funding

This study was sponsored by the Center for Individualized Medicine, Mayo Clinic, and Euroimmun.

Disclosure

J. Honorat has a patent application pending for Septin-5-IgG as biomarker of autoimmune neurologic disease. A. Lopez-Chiraboga reports no disclosures relevant to the manuscript. T.J. Kryzer has a financial interest in the following intellectual property: "Marker for Neuromyelitis Optica." A patent has been issued for this technology, and it has been licensed to commercial entities. T.J. Kryzer has received cumulative royalties of greater than the federal threshold for significant financial interest from the licensing of these technologies, but receives no royalties from the sale of these tests by Mayo Medical Laboratories. L. Komorowski and M. Scharf are employed by Euroimmun AG. S. Hinson reports no disclosures relevant to the manuscript. V. Lennon has a patent application pending for Septin-5-IgG as biomarker of autoimmune neurologic disease. She has a financial interest in the following intellectual property: "Marker for Neuromyelitis Optica." A patent has been issued for this technology, and it has been licensed to commercial entities. V. Lennon has received cumulative royalties of greater than the federal threshold for significant financial interest from the licensing of these technologies, but receives no royalties from the sale of these tests by Mayo Medical Laboratories. S. Pittock has a patent application pending for Septin-5-IgG as biomarker of autoimmune neurologic disease, and holds patents that relate to functional AQP4/NMO-IgG assays and NMO-IgG as a cancer marker; consulted for Alexion and Medimmune; and received research support from Grifols, Medimmune, and Alexion. All compensation for consulting activities is paid directly to Mayo Clinic. C. Klein reports no disclosures relevant to the manuscript. A. McKeon has a patent application pending for Septin-5-IgG as biomarker of autoimmune neurologic disease; has consulted for Grifols, Medimmune, and Euroimmun; and received research support from Grifols, Medimmune, Alexion, and Euroimmun but has not received personal compensation. Go to Neurology.org/N for full disclosures.

Publication history

Received by *Neurology* October 31, 2018. Accepted in final form April 8, 2019.

Appendix Authors

Josephe A. Honorat, MD, PhD	Data collection, analysis, and interpretation; drafting of manuscript
A. Sebastian Lopez-Chiriboga, MD	Data collection, analysis, and interpretation; critical revision of manuscript
Thomas J. Kryzer	Data collection, analysis, and interpretation; critical revision of manuscript
Lars Komorowski, PhD	Data collection and analysis; critical revision of manuscript
Madeleine Scharf, PhD	Data collection and analysis; critical revision of manuscript
Shannon R. Hinson, PhD	Data collection, analysis, and interpretation; critical revision of manuscript
Vanda A. Lennon, MD, PhD	Data collection and analysis; critical revision of manuscript
Sean J. Pittock, MD	Data collection and analysis; critical revision of manuscript
Christopher J. Klein, MD	Data collection, analysis, and interpretation; critical revision of manuscript
Andrew McKeon, MD	Study concept and design; data collection, analysis, and interpretation; drafting and critical revision of manuscript; study supervision

References

1. McKeon A, Pittock SJ. Paraneoplastic encephalomyelopathies: pathology and mechanisms. Acta Neuropathol 2011;122:381–400.
2. Dalmau J, Graus F, Rosenblum MK, Posner JB. Anti-Hu-associated paraneoplastic encephalomyelitis/sensory neuronopathy: a clinical study of 71 patients. Medicine 1992;71:59–72.
3. Lucchinetti CF, Kimmel DW, Lennon VA. Paraneoplastic and oncologic profiles of patients seropositive for type 1 antineuronal nuclear autoantibodies. Neurology 1998; 50:652–657.
4. Darnell RB, Furneaux HM, Posner JB. Antiserum from a patient with cerebellar degeneration identifies a novel protein in Purkinje cells, cortical neurons, and neuroectodermal tumors. J Neurosci 1991;11:1224–1230.
5. Honorat JA, Lopez-Chiriboga AS, Kryzer TJ, et al. Autoimmune septin-5 cerebellar ataxia. Neurol Neuroimmunol Neuroinflamm 2018;5:e474.
6. Gadoth A, Kryzer TJ, Fryer J, McKeon A, Lennon VA, Pittock SJ. Microtubule-associated protein 1B: novel paraneoplastic biomarker. Ann Neurol 2017;81:266–277.
7. Dalmau J, Tüzün E, Wu HY, et al. Paraneoplastic anti-N-methyl-D-aspartate receptor encephalitis associated with ovarian teratoma. Ann Neurol 2007;61:25–36.
8. Newman LS, McKeever MO, Okano HJ, Darnell RB. Beta-NAP, a cerebellar degeneration antigen, is a neuron-specific vesicle coat protein. Cell 1995;82:773–783.
9. Zalewski NL, Lennon VA, Lachance DH, Klein CJ, Pittock SJ, Mckeon A. P/Q- and N-type calcium-channel antibodies: oncological, neurological, and serological accompaniments. Muscle Nerve 2016;54:220–227.
10. Flanagan EP, McKeon A, Lennon VA, et al. Paraneoplastic isolated myelopathy: clinical course and neuroimaging clues. Neurology 2011;76:2089–2095.
11. Pittock SJ, Lucchinetti CF, Lennon VA. Anti-neuronal nuclear autoantibody type 2: paraneoplastic accompaniments. Ann Neurol 2003;53:580–587.
12. McKeon A, Tracy JA, Pittock SJ, Parisi JE, Klein CJ, Lennon VA. Purkinje cell cytoplasmic autoantibody type 1 accompaniments: the cerebellum and beyond. Arch Neurol 2011;68:1282–1289.
13. Newell-Litwa K, Seong E, Burmeister M, Faundez V. Neuronal and non-neuronal functions of the AP-3 sorting machinery. J Cell Sci 2007;120(pt 4):531–541.
14. Odorizzi G, Cowles CR, Emr SD. The AP-3 complex: a coat of many colours. Trends Cell Biol 1998;8:282–288.
15. Lennon VA, Kryzer TJ, Griesmann GE, et al. Calcium-channel antibodies in the Lambert-Eaton syndrome and other paraneoplastic syndromes. N Engl J Med 1995;332:1467–1474.
16. Lai M, Huijbers MG, Lancaster E, et al. Investigation of LGI1 as the antigen in limbic encephalitis previously attributed to potassium channels: a case series. Lancet Neurol 2010;9:776–785.
17. Irani SR, Alexander S, Waters P, et al. Antibodies to Kv1 potassium channel-complex proteins leucine-rich, glioma inactivated 1 protein and contactin-associated protein-2 in limbic encephalitis, Morvan's syndrome and acquired neuromyotonia. Brain 2010;133:2734–2748.
18. Salazar G, Love R, Werner E, et al. The zinc transporter ZnT3 interacts with AP-3 and it is preferentially targeted to a distinct synaptic vesicle subpopulation. Mol Biol Cell 2004;15:575–587.
19. Seong E, Wainer BH, Hughes ED, Saunders TL, Burmeister M, Faundez V. Genetic analysis of the neuronal and ubiquitous AP-3 adaptor complexes reveals divergent functions in brain. Mol Biol Cell 2005;16:128–140.
20. Evstratova A, Chamberland S, Faundez V, Toth K. Vesicles derived via AP-3-dependent recycling contribute to asynchronous release and influence information transfer. Nat Commun 2014;5:5530.
21. Assoum M, Philippe C, Isidor B, et al. Autosomal-recessive mutations in AP3B2, adaptor-related protein complex 3 beta 2 subunit, cause an early-onset epileptic encephalopathy with optic atrophy. Am J Hum Genet 2016;99:1368–1376.
22. Zhang Z, Li Q, Diao M, et al. Sporadic Hirschsprung disease: mutational spectrum and novel candidate genes revealed by next-generation sequencing. Sci Rep 2017;7:14796.
23. Wanschitz J, Hainfellner JA, Kristoferitsch W, Drlicek M, Budka H. Ganglionitis in paraneoplastic subacute sensory neuronopathy: a morphologic study. Neurology 1997;49: 1156–1159.
24. Drlicek M, Bodenteich A, Setinek U, Tucek G, Urbanits S, Grisold W. T cell-mediated paraneoplastic ganglionitis: an autopsy case. Acta Neuropathol 2000;99:599–602.
25. Plonquet A, Gherardi RK, Créange A, et al. Oligoclonal T-cells in blood and target tissues of patients with anti-Hu syndrome. J Neuroimmunol 2002;122:100–105.
26. Pereira PR, Viala K, Maisonobe T, et al. Sjögren sensory neuronopathy (Sjögren ganglionopathy): long-term outcome and treatment response in a series of 13 cases. Medicine2016;95:e3632.
27. McKeon A, Lennon VA, Pittock SJ, Kryzer TJ, Murray J. The neurologic significance of celiac disease biomarkers. Neurology 2014;83:1789–1796.

Disputes & Debates: Editors' Choice

Steven Galetta, MD, FAAN, Section Editor

Editors' note: Migraine with visual aura is a risk factor for incident atrial fibrillation: A cohort study

In "Migraine with visual aura is a risk factor for incident atrial fibrillation: A cohort study," Sen et al. followed 11,939 patients with headache and no diagnosis of atrial fibrillation for 20 years and found that after adjusting for confounders, migraine with visual aura was associated with an increased risk of atrial fibrillation. They postulated that autonomic dysfunction may be the underlying cause of both atrial fibrillation and migraine and questioned whether migraine with aura is the result of cardioembolic stroke secondary to atrial fibrillation. Gupta challenged the value of Sen et al.'s findings and commented that (1) migraine with aura and migraine without aura have the same amount of autonomic dysfunction (although no source was provided to quantify the amount of autonomic dysfunction in these 2 entities), and (2) it would be nearly impossible for thromboembolic events due to atrial fibrillation to serially occur in the same cerebrovascular territory leading to migraine with aura. In response, Sen (1) replied that migraine with aura and migraine without aura are commonly considered to be distinct entities and pathophysiologic variants and cited a document published by the International Headache Society and (2) cited a review article that concluded that migraine with aura tends to produce more significant autonomic impairment than migraine without aura. In addition, Sen reinforced that there is a relationship between both (1) migraine with aura and atrial fibrillation (as shown in the present study) and (2) ischemic stroke and migraine with aura (as shown in a previous study). However, it remains unclear whether autonomic dysfunction is responsible for, or merely related to, migraine. Last, Hsieh noted that the x-axis of the Kaplan-Meier curves showing 20-year outcome of incident atrial fibrillation in figure 1 should be labeled "Time to atrial fibrillation," not "Time to stroke," and that the log-rank p value of 0.0048 shown on the figure is different from that which is noted in the text ($p = 0.0002$). Sen replied that Hsieh is correct that the x-axis label should be changed, but said that the p value in the figure is correct (and did not clarify why it is different from the p value in the text).

Ariane Lewis, MD, and Steven Galetta, MD
Neurology® 2019;93:645. doi:10.1212/WNL.0000000000008203

Reader response: Migraine with visual aura is a risk factor for incident atrial fibrillation: A cohort study

Vinod Gupta (New Delhi)
Neurology® 2019;93:645–646. doi:10.1212/WNL.0000000000008202

I read with interest the article by Sen et al.[1] The investigators believe that migraine with aura (MwA) and migraine without aura (MwoA) are distinct clinical entities. Neuropharmacologically, both beta-blockers and tricyclic antidepressants are equally effective in the prevention of both variants. This study[1] does not distinguish between variants of migrainous visual aura.[2] Only the migrainous visual field loss without scintillation can be conceived of as being of ischemic origin. The pathognomonic scintillating scotoma was not seen in any patient.[1] Retrospective questionnaire responses for migrainous visual aura are highly subjective.

Author disclosures are available upon request (journal@neurology.org).

Recurrent stereotyped MwA-headache attacks of atrial fibrillation (AF)-related thromboembolism require the presumed passage of vascular-occluding substance(s) into the same cranial vascular territory, predictably or unpredictably, over decades—a highly unlikely to impossible clinical scenario.[3] AF begins in the right atrium. The pulmonary circulation cannot remain indefinitely spared in patients with MwA-AF. There is also no difference in autonomic dysfunction between patients with MwA and patients with MwoA, as speculated.[1]

Meta-analysis obtains bizarre associations and has introduced a façade of mathematical acceptability that draws the clinician away from reality.[4] The linkage of AF-related presumed thromboembolism to patients with MwA,[1] despite lack of commonsense and logic in closure of the patent foramen ovale to prevent migraine attacks,[3] appears to be misplaced.

1. Sen S, Androulakis XM, Duda V, et al. Migraine with visual aura is a risk factor for incident atrial fibrillation: a cohort study. Neurology 2018;91:e2202–e2210.
2. Hupp SL, Kline LB, Corbett JJ. Visual disturbances in migraine. Surv Ophthalmol 1989;33:221–236.
3. Gupta VK. Patent foramen ovale closure and migraine: science and sensibility. Expert Rev Neurother 2010;10:1409–1422.
4. Horton RC, Kendall MJ. Clinical pharmacology and therapeutics. Postgrad Med J 1991;67:1042–1054.

Reader response: Migraine with visual aura is a risk factor for incident atrial fibrillation: A cohort study

Cheng-Yang Hsieh (Tainan, Taiwan)
Neurology® 2019;93:646. doi:10.1212/WNL.0000000000008210

In figure 1,[1] the x-axis should be "Time to incident atrial fibrillation" rather than "Time to stroke." Besides, the "log-rank *p* value" in figure 1 was not consistent with that in the text (paragraph 2, page e2205). Please check.

1. Sen S, Androulakis XM, Duda V, et al. Migraine with visual aura is a risk factor for incident atrial fibrillation: a cohort study. Neurology 2018;91:e2202–e2210.

Author response: Migraine with visual aura is a risk factor for incident atrial fibrillation: A cohort study

Souvik Sen (Columbia, SC)
Neurology® 2019;93:646–647. doi:10.1212/WNL.0000000000008211

I thank Dr. Gupta for the comment on our article.[1] Migraine with aura is considered a different clinical entity compared with migraine without aura.[2] Pathophysiologically, the 2 are considered to be variants, with the accepted notion being that visual aura is generated by cortical spreading depression.[3] We have shown that migraine with aura is a risk factor for ischemic stroke of cardioembolic subtype.[4] The migraine questionnaire was administered through a structured interview by trained personnel, similar to what a clinician may achieve at the bedside to make migraine with and without aura diagnoses. Studies have shown that migraine with aura is associated with autonomic dysfunction.[5]

I also wish to thank Dr. Hsieh for identifying the typographical errors in our article.[1] In figure 1, the x-axis label should be "Time to incident atrial fibrillation" rather than "Time to stroke." However, the "log-rank *p* value" in figure 1 is correct (0.0048).

Author disclosures are available upon request (journal@neurology.org).

1. Sen S, Androulakis XM, Duda V, et al. Migraine with visual aura is a risk factor for incident atrial fibrillation: a cohort study. Neurology 2018;91:e2202–e2210.
2. Headache Classification Committee of the International Headache Society (IHS) the International Classification of Headache Disorders, 3rd edition. Cephalalgia 2018;38:1–211.
3. Vgontzas A, Burch R. Episodic migraine with and without aura: key differences and implications for pathophysiology, management, and assessing risks. Curr Pain Headache Rep 2018;22:78.
4. Androulakis XM, Kodumuri N, Giamberardino LD, et al. Ischemic stroke subtypes and migraine with visual aura in the ARIC study. Neurology 2016;87:2527–2532.
5. Miglis MG. Migraine and autonomic dysfunction: which is the horse and which is the jockey? Curr Pain Headache Rep 2018;22:19.

CORRECTIONS

Autoimmune gait disturbance accompanying adaptor protein-3B2-IgG

Neurology® 2019;93:647. doi:10.1212/WNL.0000000000008232

In the article "Autoimmune gait disturbance accompanying adaptor protein-3B2-IgG" by Honorat et al.,[1] first published online August 1, 2019, the legend for figure 2 should have read "(A) Control CSF from normal pressure hydrocephalus patient and (B) healthy control serum do not bind to the surface of living hippocampal neurons. Neither CSF (D) nor serum (E) from patients 1–10 (representative images from patient 5) bind to the neuronal cultures. In contrast, NMDAR-IgG-positive patient CSF binds in a punctate pattern to the extracellular surface of hippocampal neurons (C, green). Cells were poststained for acetylated tubulin to identify axons (F, red). Nuclei stained with DAPI in all panels (white). Scale bar, 20 μm." The corrected version appeared in the September 3 issue. The authors regret the error.

Reference

1. Honorat JA, Lopez-Chiriboga AS, Kryzer TJ, et al. Autoimmune gait disturbance accompanying adaptor protein-3B2-IgG. Neurology 2019;93:e954–e963.

Clinical trials of disease-modifying agents in pediatric MS

Opportunities, challenges, and recommendations from the IPMSSG

Neurology® 2019;93:647. doi:10.1212/WNL.0000000000008186

In the article "Clinical trials of disease-modifying agents in pediatric MS: Opportunities, challenges, and recommendations from the IPMSSG" by Waubant et al.,[1] first published online May 1, 2019, the Coinvestigator appendix—the list of those who reviewed and approved the consensus statement—should have included Investigators Angelo Ghezzi (Centro Studi Sclerosi Multipla, Ospedale di Gallarate, Gallarate, Italy), Amit Bar-Or (Center for Neuroinflammation and Experimental Therapeutics and the Department of Neurology, University of Pennsylvania, Philadelphia, PA), and Andrew Kornberg (University of Melbourne, Parkville, Australia), who each reviewed the manuscript. The authors regret the errors.

Reference

1. Waubant E, Banwell B, Wassmer E, et al. Clinical trials of disease-modifying agents in pediatric MS: opportunities, challenges, and recommendations from the IPMSSG. Neurology 2019;92:e2538–2549.

Author disclosures are available upon request (journal@neurology.org).